JCAMECH
Vol. 46, No. 2, July 2015, pp 167- 175

Numerical Study of Droplet Generation Process in a Microfluidic Flow Focusing

Ali Lashkaripour[1], Ali Abouei Mehrizi[1*], Mohammadreza Rasouli[1] and Masoud Goharimanesh[2]

1. Department of Life Science Engineering, University of Tehran, Tehran, Iran

2. Mechanical Engineering Department, Ferdowsi University of Mashhad, Mashhad, Iran

Received 16 April 2015; Accepted 18 June 2015

Abstract

Microfluidic flow focusing devices have been utilized for droplet generation on account of its superior control over droplet size. Droplet based microfluidics addressed many scientific issues by providing a novel technological platform for applications such as biology, pharmaceutical industry, biomedical studies and drug delivery. This study numerically investigated the droplet generation process of an aqueous flow in oleic acid oil in a microfluidic flow focusing device. A conservative level set method is conducted to numerically model the droplet generation process. The post processing of the simulation results are done using Canny edge detection image processing method, which is a novel approach. Moreover, the results of the numerical simulation were compared to the experimental data provided by Ten et al. on the same device. This method showed a maximum average deviation from the experimental results of 14.6% and a minimum of 6.96%. Also, by means of altering water and oil flows, the influence of parameters affecting droplet size, which lead to a better understanding of droplet generation phenomenon, was investigated in this study. Therefore, it can be concluded that the flow ratio and capillary number are the two primary parameters that affect droplet size, while capillary number showed more dominance in comparison to flow ratio.

Keywords: *computational fluid dynamics (CFD), droplet generation, flow focusing, level set, microfluidic.*

1. Introduction

The microfluidic technology associated with Lab on a Chip (LOC) devices and micro-total analysis systems (μTAS) has experienced an eye-catching development. This technology is aimed to revolutionize the medical, pharmaceutical, healthcare and chemical industries [1]. Microfluidic devices provide several advantages such as quick results, high-throughput analysis and low consumption of reagents, which will result in low cost in comparison to conventional methods. Moreover, the energy and time required for the fabrication of microfluidic devices also in operation energy consumption are significantly reduced, compared to conventional devices[2]. Typically, microfluidic devices can fall into two categories, continuous and droplet based

* Corresponding author Email: abouei@ut.ac.ir

microfluidic devices. In the first type, a continuous stream line of fluid is enclosed in a microchannel bounded by the channel's walls. In such devices, micro-valves and micro-pumps are often needed for manipulating and controlling the continuous fluids. These microfluidic systems are readily made and controlled. However, the reliability of its components, their micromachining cost, low energy efficiency and its relatively complicated packing process still remains challenging [3]. Alternatively, droplet based microfluidic systems are capable of moving and manipulating discrete droplets compared to a continuous flow. The primary goal of droplet based microfluidics is the possibility of creating small components, sought after in order to produce moderate volume of fluids with highly controlled shape, size and properties [4]. Certain LOC devices, such as droplet based reactors, have drawn several attention to the field of digital biology, with applications such as single-cell analysis and single-copy nucleic acid analysis, which includes multiplexed digital PCR, monoclonal template amplification for bead-based gene sequencing, digital quantification of DNA and reverse transcriptase (RT-PCR) for the detection of single RNA fragments [5]. Droplet based microfluidic devices can produce highly uniform shaped and sized droplets within the range of 10-100 µm in diameter with less than 5% size deviation [6]. This precise droplet generation roots, in confinement of the ejected droplet into a Laminar and low Reynolds number flow, resulted from the micro-scale geometries [7]. Since the droplet interface plays same role as membrane confinement of contents (inside), discretization of certain fluid within a second flow has become specifically appealing for gaining a superior control over reactions [8]. To evaluate this concept, two phase flows were utilized in order to optimize the biochemical reactions including polymerase chain reaction (PCR) for gene expression and its analysis. Also, emulsion concept was adopted with the aim of gaining a precise control over drug delivery rates [9]. The diameters of the droplets generated in microfluidic flow focusing (MFF) devices follows same order in comparison to the orifice size, which becomes appealing in certain biological applications, such as detection of rare DNA sequences in PCR chips that can result to early cancer detection [10]. Several parameters affect the process of droplet formation including flow rates, viscosity, Capillary number, surface tension and geometric parameters. Several experimental studies have been carried out on the droplet generation process in Microfluidic devices [6, 7, 11]. The droplet producing process is yet to be fully understood due to its dependence on large number of independent parameters [12]. Therefore, numerical study of this process has draws the attention of many to the subject.

Computational fluid dynamics (CFD) simulations could be used as an alternative tool to understand the unknown and complicated physics that govern this process. The challenge in a numerical model is not entirely reliable until it is verified using experimental data. Several, researchers have attempted to clarify the physics of this phenomena adopting numerical methods [4, 12, 13]. However, some studies showed a deviation of 60% from the experimental data in approximating the droplet radius [4].

The aim of this study was to determine the droplet generation process in a microfluidic flow focusing (MFF) device by proposing an accurate numerical model of the regarded process. Moreover, when the experimental results obtained from the study of Tan et al. were compared, this study's numerical model was verified. Therefore, this study numerically investigated the process using water as the dispersed phase and Oleic acid oil as the continuous phase in a microfluidic droplet generation device.

2. Materials And Methods

2.1. Geometry of MFF device

The geometry of the microfluidic flow focusing device was adopted from Tan et al. study [14]. As clarified by Tan et al. this geometry is superior to conventional flow focusing geometries due to its capability of creating mono-dispersed droplets and certain droplet breaking point due the velocity field created by nozzle. As shown in Figure 1, water was designated as the discrete phase, which is injected into the MFF device via the central 48 µm wide channel and oleic acid as the continuous phase was fed to the system

through double 48 μm wide, side channels. As the two phases meet in the pressure reservoir, they tend to be pushed through an orifice with a width of 48 μm. In the downstream of the orifice, the width of channel tend to increase from 48 to 230 μm in a length of 322 μm and the outlet channel has a constant width of 50 μm for an 80 μm length.

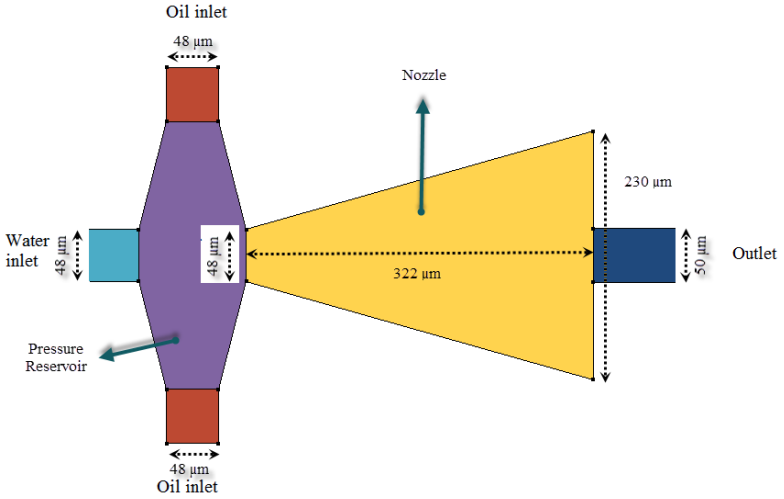

Fig. 1. Geometry of microfluidic flow focusing device adopted from Tan et al. study [14]

The properties of the two fluids are shown in Table 1. The properties of oleic acid were inserted manually to COMSOL and were directly obtained from the data provided by Tan et al. [14].

Table 1. Fluid properties used in the simulation

Fluid	Density [kg/m^3]	Viscosity [N.s/m^2]	Surface Tension [N/m]
Water	1000	8.90×10^{-4}	0.0156
Oleic acid	895	0.02764	

2.2. Numerical setup

Level-set method (LS) and volume of fluid (VOF) method are typically utilized in order to model two phase flows [15]. VOF method adopts the volume fraction equation and considers the geometric construction aimed to evaluate the weighted density and viscosity in each computational mesh. However, the VOF inherently conserves the mass, nevertheless, the interface of fluids is not precisely calculated which produces error in the evaluation of interfacial forces. In microfluidic devices with a micro scale orifice, the inaccurately captured interface could result in large error if the generation of droplet was modeled utilizing the VOF method. LS method, on the other hand, captures the interface by a smooth function and it is very convenient for calculating the curvature and surface tension forces. Therefore, LS is more advantageous in modeling the droplet generation process inside a microfluidic device [12].

The governing equations of the flow include continuity equation (1) and the incompressible Navier-Stokes equation (2):

$$\frac{\partial \rho}{\partial t} + \nabla.\left(\rho \vec{u}\right) = 0 \tag{1}$$

$$\frac{\partial \left(\rho \vec{u}\right)}{\partial t} + \nabla.\left(\rho \vec{u}\vec{u}\right) = -\nabla P + \nabla.\left[\mu\left(\nabla \vec{u} + \nabla \vec{u}^{T}\right)\right] + \vec{F} \tag{2}$$

where ρ is the fluid density, $\vec{u}$ is the velocity field and $\vec{F}$ is the volume body force. As a result of the low density difference between the two phases, and small masses and velocities, the gravitational force is neglected; therefore, $\vec{F}$ only consists of the interfacial tension force. In this study, the conservative level set method developed by Olsson and Kreiss [16] is conducted to simulate the droplet generation process. The inherent mass conservation problem of the classical LS method is addressed by the conservative form of LS method. The LS equation is given in Equation (3):

$$\frac{\partial \varnothing}{\partial t} + \vec{u}.\nabla \varnothing = \gamma \nabla.\left(\epsilon \nabla \varnothing - \varnothing\left(1-\varnothing\right)\frac{\nabla \varnothing}{\left|\nabla \varnothing\right|}\right) \tag{3}$$

where ϕ is the level set function that ranges from 0 to 1. When ϕ<0.5 in a certain mesh, then the regarded mesh is considered as phase 1; whereas ϕ>0.5, indicates that the mesh is filled with phase 2. γ and ε are the parameters of stabilization, where γ indicates the amount of re-initialization of the level set function. The maximum value that velocity field $\vec{u}$ takes, is considered to be a suitable value for γ. As shown in Figure 2, by analyzing the velocity distribution, the value of γ could be determined. ε sets the thickness of the interface, while ϕ varies smoothly from 0 to 1. The ε parameter must be chosen to ensure that it has the same order as the interfacial mesh size.

Thereafter, the interfacial variables such as the unit normal to the interface $\hat{n}$ and the curvature κ, could be evaluated using the relations given in Equations (4) and (5), respectively:

$$\hat{n} = \frac{\nabla \varnothing}{|\nabla \varnothing|} \tag{4}$$

$$\kappa = -\nabla . n \,|_{\varnothing=0.5} \tag{5}$$

The surface tension force exerted on the interface of the two phases is calculated using the relation given in Equation (6):

$$\vec{F}_{sf} = \sigma \kappa \delta \hat{n} \tag{6}$$

where σ is the interfacial tension coefficient with a unit of (N/m), although, in this study, σ is considered to have a constant value of 0.0156 N/m, and κ is the curvature as shown in Equation (5). δ is a Dirac delta function that is concentrated to the interface of two phases. δ smooth function approximation is given in Equation (7).

$$\delta = 6|\nabla \varnothing||\varnothing(1-\varnothing)| \tag{7}$$

Also, viscosity μ and the density ρ in Equation (3) are smoothed by ϕ across the interface as shown in Equations (8) and (9), respectively:

$$\mu = \mu_1 + (\mu_2 - \mu_1)\varnothing \tag{8}$$

$$\rho = \rho_1 + (\rho_2 - \rho_1)\varnothing \tag{9}$$

2.3. Implementation in the COMSOL Environment

In the Two-Phase flow, the level set for the CFD module in COMSOL Multiphysics 4.4 is used for the numerical simulations. The simulations are carried out in a two dimensional domain, and the geometric dimensions are shown in Figure 1. The flows were modeled as incompressible Newtonian fluids, also, the inertial terms were neglected due to low velocity and mass of the flows (Stokes flow). The channel walls were considered as wetted wall condition with a constant contact angle of 3π/4 rad. for all the cases. γ was inserted manually by studying the velocity field, γ takes the maximum value of velocity, for instance, if Q_w= 0.3 μL/min and Q_o= 1 μL/min, then γ= 0.01 m/s.

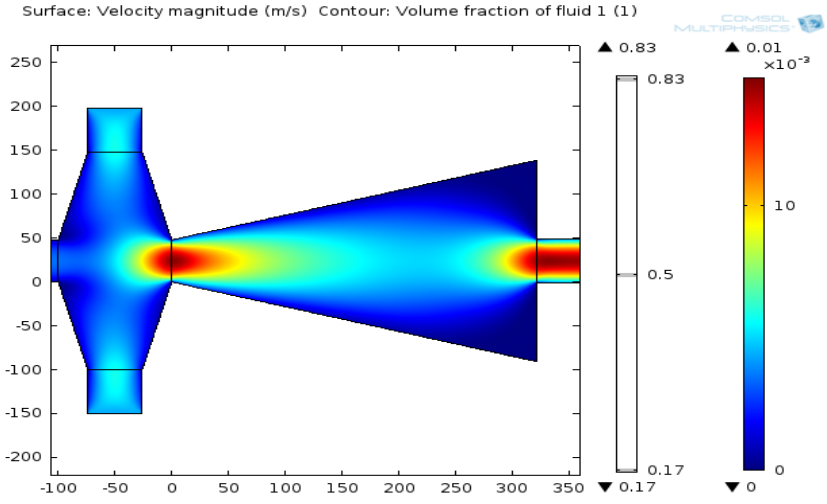

Fig. 2 Velocity distribution by applying Q_w=0.3 μL/min and Q_o=1 μL/min

After performing grid dependence studies with different grid resolutions, a numerical mesh that consists of 9622 domain triangular elements and 481 boundary triangular elements was adopted in this study as shown in Figure 3.

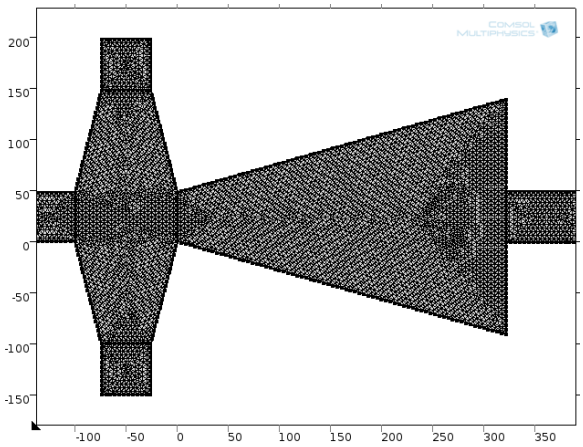

Fig. 3. The geometry and mesh in numerical simulation

2.4. Image processing

In order to validate the numerical simulation, the simulation results were compared to the experimental results given in Tan et al. study[14]. The validation process was conducted by utilizing the image processing tool in MATLAB environment. This validation was completed by edge detection.

The boundary that distinguishes the object aimed to be extracted and the background is called an edge. Therefore, edge tends to separate the object from the background. Moreover, apart from the object intended to be detected, the background is of great practical significance for further processing of several applications, such as face recognition, image segmentation, and image enhancement. As a result, effective improvement of the accuracy of edge detection is crucial. In order to detect the droplet accurately in a background of oil, it is necessary to first detect and extract an accurate edge. Traditional edge detection methods utilize Roberts operator, Sobel operator, Prewitt operator and LOG operator. All aforementioned operators are local window gradient operators, which are appealing because of their simple structure and fast detection. On the other hand, they are more affected by noise [17] and as a result, these methods are not entirely satisfactory in practical applications. In 1986, John Canny proposed the Canny criterion and based on this criterion, he proposed an optimal edge detection operator (Canny operator [18]). The regarded algorithm is based on the optimization algorithm, which is beneficial due to its greater signal to noise ratio (SNR) and precise detection progress in comparison to traditional methods. In this regard, several experiments were conducted to prove that Canny operator's edge detection is superior to other traditional detection operators when the image was polluted by Gaussian white noise.

Therefore, in this study, in order to accurately detect the droplet from its background, Canny algorithm was conducted. The results and data of 19 conducted experiments made available by Tan et al. [14] were simulated, and their snapshots were processed utilizing Canny's algorithm. A sample snapshot of the numerical solution output of an experiment done by Tan et al. is shown in Figure 4. As shown in Figure 4, ϕ varies from 0 to 1, and the boundary between the green ring (definitely oil) and the dark blue ring (definitely water) represents the interface between oil and water. Therefore, by detecting these two rings and calculating their diameter, an average of these diameters could be a satisfactory approximation for the droplet diameter.

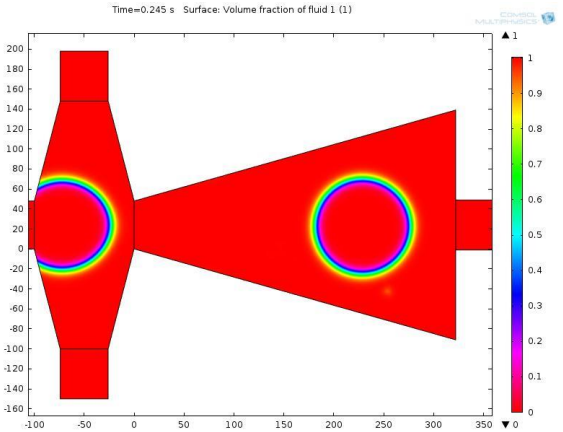

Fig. 4. Simulation result of droplet generation, Q_o=1 and Q_w=0.3

3. Results And Discussion

All 19 simulations were processed using the Canny algorithm. Figure 5 shows all snap shots after and before image processing. For each of these numerical solutions, three numbers are given, the first one represents the water flow in

µL/min, the second number represents the oil flow in µL/min and the last one indicates the diameter of the droplet approximated by Canny image processing algorithm.

Because of the confinement caused by the shape of the upper and lower walls, the generated droplets in the nozzle are compressed by the microchannel. As a result, these droplets have a larger apparent diameter in comparison to the diameter of spherical droplets that are not compressed with equal volume. It is crystal clear that, in channel (disc), the diameter of droplet is always larger than the diameter of a spherical droplet with the same volume. By observing this, Tan et al. proposed Equation (10) to relate the disc radius to the spherical radius [14].

$$r_d = 0.5136 r_s^{1.2817} \tag{10}$$

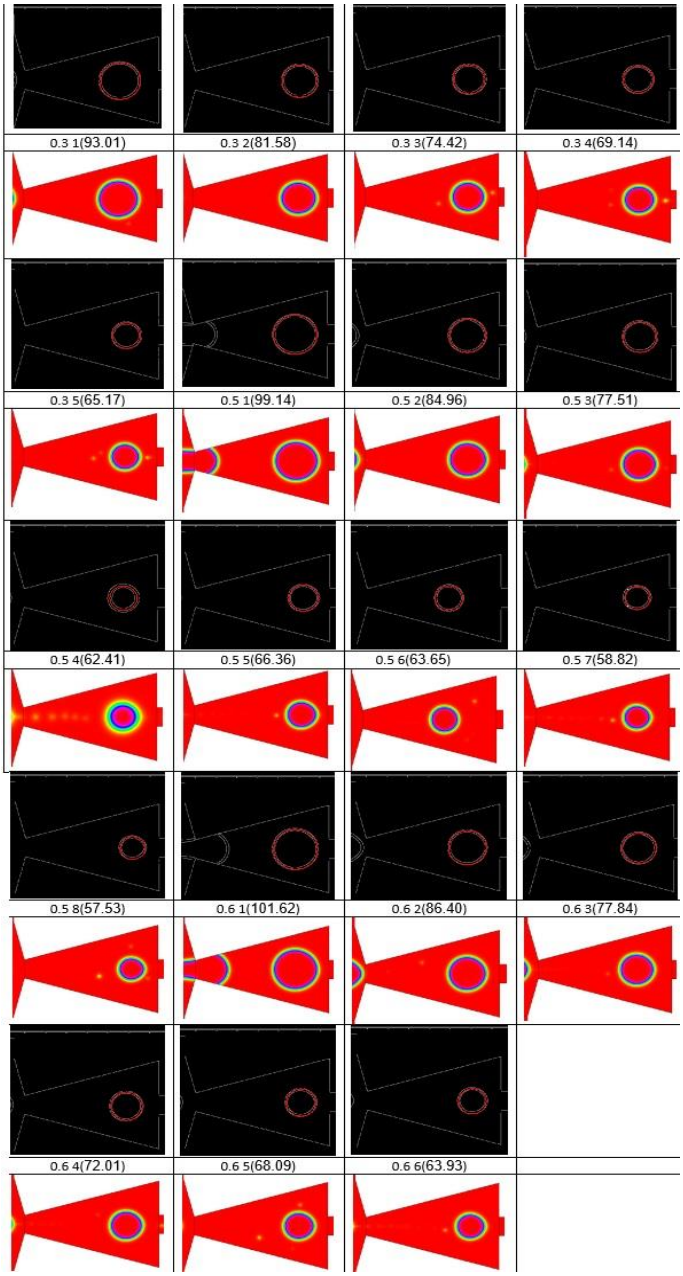

Fig. 5. Calculating the disc diameter using Canny algorithm in MATLAB environment for different oil and water flows. Each dark image represents the processed image of the snapshot below it. Between each processed image and snapshot, three numbers are given, the first and second represent the water and oil flow in µL/min and the last number indicates the diameter of the droplet approximated by Canny algorithm.

Based on data from the previous step, the diameter of the disc droplet were calculated, and by using Equation (10) the radius of the sphere droplet was calculated. The simulation results and the experimental data are compared as shown in Figure 6.

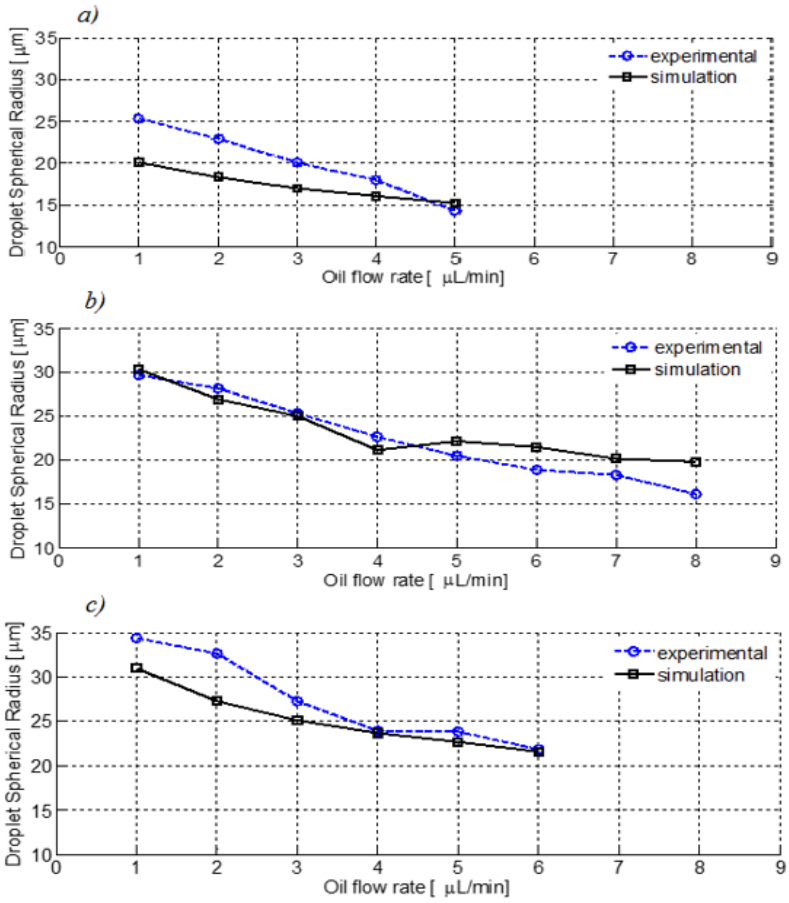

Fig. 6. Comparison of experimental and numerical results for different oil and water flow rates

As elucidated in Figure 6, the numerical solutions showed the same behavior and pattern to experimental results. Although, at lower flows, the simulation showed some deviations from the experiments, and at greater flows, it matched the data more accurately. The numerical solution showed an average error of 14.6% for Q_w=0.3, 8.63% for Q_w=0.5 and 6.96% for Q_w=0.6%. The relation used to calculate average error is given in Equation (11):

$$Average\ Error = \frac{\sum_1^n \frac{D_s - D_e}{D_e}}{n} \times 100 \qquad (11)$$

where n is the number of experiments, D_s is simulation droplet diameter and D_e is experimental droplet diameter.

Some snapshots of droplet breaking process of the flow focusing device provided by Tan et al. [14] are shown in Figure 7a. These snapshots were created again by utilizing the numerical modeling. The results show promising accuracy of numerical modeling, the simulated snapshots of breaking process are indicated in Figure 7b.

Figure 7, proves that the numerical solution does not only precisely simulates the breaking process, but also, it accurately modeled the production of satellite droplets. Figures 6 and 7 show the quantitative agreement between the experiments and the numerical simulation at various flows of oil and water. The numerically calculated droplet radius are well matched with the experimental data, which suggests accurate modeling of the droplet formation and precise image processing. With the proven accuracy of the numerical model, further study on the droplet generation process is required.

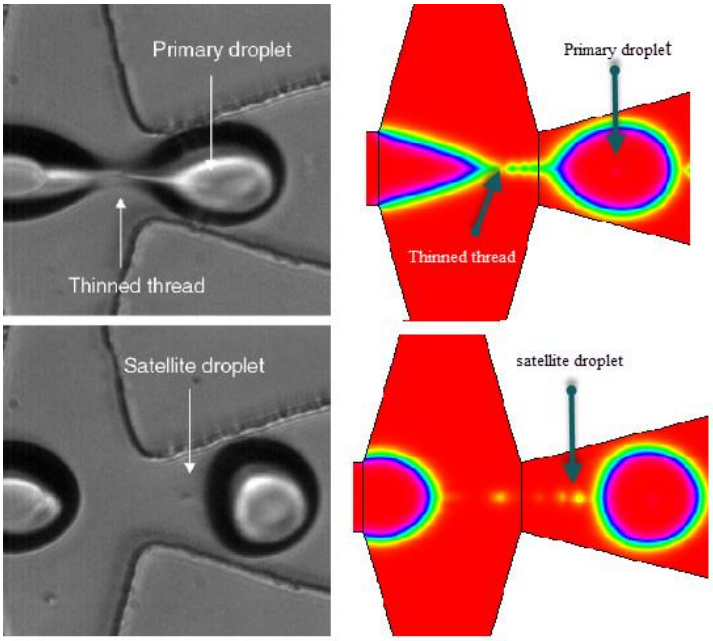

Fig. 7. Comparison of the experimental and simulation results in droplet breaking process a (left). Snapshots of experiments done by Tan et al. [14] b. (right) Snapshots of simulations

The results are discussed in terms of flow ratio of the continuous flow (oleic acid oil) to the discrete flow (water) (Q_o/Q_w), where Q_o is the oil flow and Q_w the water flow rate.

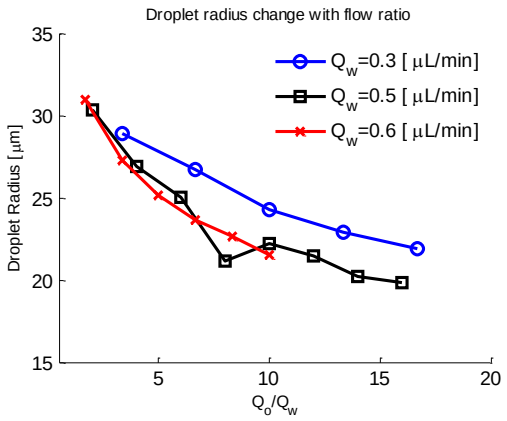

Fig. 8. Droplet radius change with flow ratio

Figure 8 clarifies that the droplet radius decreases with increase of flow ratio. Consequently, a smaller water flow and a greater oil flow rate would lead to production of a droplet with smaller size. Figure 8 also shows that discrete flow rate has minor effect on droplet radius and the flow ratio is the primary parameter in determining the droplet size. Thus, the results could be discussed in terms of capillary number (Ca), based on the continuous phase. The Ca number is given in Equation (12):

$$Ca = \frac{\mu_c u_c}{\sigma} \tag{12}$$

where μ_c is the dynamic viscosity of the continuous phase, u_c is the velocity of continuous phase and σ is the surface or interfacial tension between the two fluid phases.

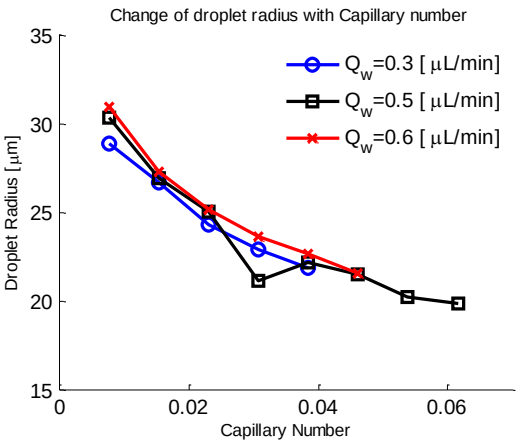

Fig. 9. Droplet radius change with capillary number

Figure 9 indicates that the droplet size decreases with an increase of the capillary number. Therefore, more viscous oil and a greater oil flow will result in smaller droplet. It

also shows that the capillary number is another primary parameter in the determination of droplet radius. Droplet radius shows a negligible deviation with change in water flow rate for a certain capillary number. By comparing Figures 8 and 9, it becomes obvious that capillary number is a more dominant parameter that affects the droplet size in comparison to flow ratio. The dominance of capillary number also reveals the importance of the surface tension, which could be altered using surfactants. Therefore, by adding a certain surfactant that cause variation of surface tension, droplet size could be controlled needless of an alteration in flows parameters, such as flow rates and viscosity.

4. Conclusion

The droplet formation process in a microfluidic flow focusing device was studied numerically by conducting the conservative level set method in COMSOL Multiphysics environment. Graphic results of the simulations were processed using Canny edge detection algorithm to determine the droplet diameter. The numerical solution results showed excellent qualitative and quantitative agreement with the experimental data provided by Tan et al. which validated the modeling method. It was shown that the accuracy of numerical solution increases with water flow rate, the average error decreased from 14.6 to 6.96% by increasing the water flow rate from 0.3 to 0.6 μL/min. Afterwards, droplet radius variation with flow ratio and capillary number was studied. It was clarified that these two parameters were the primary parameters affecting droplet size, rather than water flow and oil flow singularly. Finally, it was shown that capillary number is more dominant in determining the droplet radius in comparison to flow ratio.

References

[1].Zhang, C., et al. (2006). *PCR microfluidic devices for DNA amplification.* Biotechnology advances, 24(3): p. 243-284.

[2].Zhang, Y., Ozdemir, P. (2009). *Microfluidic DNA amplification—a review.* Analytica chimica acta, 638(2): p. 115-125.

[3].Chang, Y.H., et al. (2006). *Integrated polymerase chain reaction chips utilizing digital microfluidics.* Biomedical microdevices, 8(3): p. 215-225.

[4].Granado, K.V.R., et al. (2013). *Numerical simulation of droplet formation in a microchannel device.* The International Journal of Multiphysics, 7(4): p. 271-286.

[5].Hatch, A.C., et al. (2011). *1-Million droplet array with wide-field fluorescence imaging for digital PCR.* Lab Chip, 11(22): p. 3838-3845.

[6].Nie, Z., et al. (2008). *Emulsification in a microfluidic flow-focusing device: effect of the viscosities of the liquids.* Microfluidics and Nanofluidics, 5(5): p. 585-594.

[7].Lee, W., L.M. Walker, Anna, S.L. (2009). *Role of geometry and fluid properties in droplet and thread formation processes in planar flow focusing.* Physics of Fluids (1994-present), 21(3): p. 032103.

[8].Christopher, G., Anna, S. (2007). *Microfluidic methods for generating continuous droplet streams.* Journal of Physics D: Applied Physics, 40(19): p. R319.

[9].Griffiths, A.D., Tawfik, D.S. (2006). *Miniaturising the laboratory in emulsion droplets.* Trends in biotechnology, 24(9): p. 395-402.

[10]. Anna, S.L., Bontoux, N., Stone, H.A. (2003). *Formation of dispersions using "flow focusing" in microchannels.* Applied physics letters, 82(3): p. 364-366.

[11]. Garstecki, P., Stone, H.A. Whitesides, G.M. (2005). *Mechanism for flow-rate controlled breakup in confined geometries: A route to monodisperse emulsions.* Physical Review Letters, 94(16): p. 164501.

[12]. Li, Y., Jain, M., Nandakumar, K. (2012). *Numerical study of droplet formation inside a microfluidic flow-focusing device*. in *COMSOL Conference Proceeding*.

[13]. Conneely, M., et al. *Computationally Assisted Design and Experimental Validation of a Novel'Flow-Focussed'Microfluidics Chip for Generating Monodisperse Microbubbles.*

[14]. Tan, Y.C., Cristini, V. Lee, A.P. (2006). *Monodispersed microfluidic droplet generation by shear focusing microfluidic device.* Sensors and Actuators B: Chemical, 114(1): p. 350-356.

[15]. Liu, J., Nguyen, N.T. (2010). *Numerical simulation of droplet-based microfluidics.*

[16]. Olsson, E., Kreiss, G. (2005). *A conservative level set method for two phase flow.* Journal of computational physics, 210(1): p. 225-246.

[17]. Basu, M. (2002). *Gaussian-based edge-detection methods-a survey.* IEEE Transactions on Systems, Man, and Cybernetics, Part C, 32(3): p. 252-260.

[18]. Canny, J. (1986). *A computational approach to edge detection.* Pattern Analysis and Machine Intelligence, IEEE Transactions on, (6): p. 679-698.